An analysis of the NEXAFS spectra of a molecular crystal: α-glycine — Source link ⧉

Craig P. Schwartz, Richard J. Saykally, David Prendergast

Institutions: University of California, Berkeley, Lawrence Berkeley National Laboratory

Published on: 27 Jul 2010 - Journal of Chemical Physics (American Institute of Physics)

Topics: Spectral line

Related papers:

- Innershell absorption spectroscopy of amino acids

- pH dependence of the electronic structure of glycine.

- Local Electronic Structure of Functional Groups in Glycine As Anion, Zwitterion, and Cation in Aqueous Solution

- Effects of vibrational motion on core-level spectra of prototype organic molecules

- X-ray Absorption Spectra Of Water From First Principles Calculations

An Analysis of the NEXAFS Spectra of a molecular crystal: α-Glycine

Craig P. Schwartz[1,2], Richard J. Saykally[1,2], David Prendergast[3]*

1. Department of Chemistry, University of California, Berkeley

2. Chemical Sciences Division, Lawrence Berkeley National Laboratory

3. Molecular Foundry, Lawrence Berkeley National Laboratory

* Corresponding Author - E-mail: dgprendergast@lbl.gov

Phone : (510) 486-4948

Fax : (510) 486-7424

Abstract

     The nitrogen K-edge Near Edge X-ray Absorption Fine Structure (NEXAFS) spectrum of α-crystalline glycine has been calculated for temperatures ranging from 0 K to 450 K. Significant temperature dependent spectral changes are predicted. The calculated room temperature spectrum is in good agreement with experiment. At high temperatures, molecular motions strongly influence the spectrum, as any unique spectrum from an individual instantaneous configuration does not resemble the experimental result or the average calculated spectrum; complex coupled motions in this prototypical molecular crystal underlie the observed spectral changes.

1. Introduction

Seeking to understand electronic structure and geometrical structures of biological molecules, much research has addressed amino acids using Near Edge X-ray Absorption Fine Structure (NEXAFS) spectroscopy.[1-18] These studies began with single amino acids, and progressed to dipeptides, wherein it was noted that the formation of a peptide bond causes significant spectral changes.[4,7,15,18] The belief that one could use a "building block" approach to untangle the spectra of proteins was a large driving force behind this approach, viz. that one should be able to predict a protein spectrum given the amount and type of each amino acid with an appropriate spectral library and proper accounting for the peptide bond.[19] While this approach has shown modest success, the calculated spectra of polypeptides and proteins should be considered a first approximation.[20-22] In this paper, we address the origins of the spectral features of the molecular crystal α-glycine, and how this relates to protein NEXAFS spectra.

Although nitrogen K-edge spectra of glycine (solid, s) have been obtained with widely differing results, most likely due to sample preparation issues, the literature has converged on a single "correct" solid glycine spectrum.[4,11,15-18] This spectrum is dominated by a single peak centered at 406.8 eV, assigned to N 1s $\rightarrow$ σ* $_{(N-C)}$ and N 1s $\rightarrow$ σ* $_{(N-H)}$ transitions.[4,11,15-18] There have been assignments made for low energy shoulders and a feature well above the main peak in energy, however, the latest data indicates a single strong spectral peak, although it is not Gaussian and is almost certainly due to a superposition of transitions.[17]

While there are several crystalline forms of glycine, α-glycine is both the form in which glycine readily crystallizes and also the most stable under standard laboratory conditions.[23] The structure has been determined by x-ray diffraction, neutron diffraction and using X-N difference Fourier methods.[23-28] The crystal structure does not change significantly with temperature,

experiencing less than a 1.7% change in any of the unit cell parameters over the almost 500K range which has been studied.[29] Glycine (NH_2CH_2COOH) is zwitterionic in its crystalline form, i.e., the NH_2 group becomes an NH_3^+ and the COOH group becomes COO^-.[4,11,15-18] This is similar to the form found when solvated in water, but different from that in the gas phase.[8,12] The N K-edge spectra are largely unchanged between crystalline glycine and glycine chloride (s), a protonated form of glycine where the NH_3^+ group remains, but changes drastically upon being switched to sodium glycinate (s), where the NH_3^+ group becomes an NH_2 group.[4,11,15,17,18] The N K-edge spectrum of zwitterionic glycine (s) exhibits a single peak centered at ~407 eV in energy, but when the NH_2 group is present several prominent features appear before the major peak at approximately ~402 eV.[11] This low energy feature at ~402 eV has also been observed for glycine in its aqueous anionic form, as well as for several related glycine(s) structures wherein the structure is terminated with an NH_2 group. A low energy feature is also seen in the glycine dipeptide, gly-gly.[4,11,15,17,18] The gas phase spectrum of glycine(g), which is terminated in an NH_2 group, is significantly different from the solid forms of glycine even when they are terminated with an NH_2 group.[12] It has been noted previously that the condensed phase spectrum of glycine(s) is different from that of the gaseous phase largely due to either the conversion or quenching of spatially extended Rydberg states in the gas to excitons in the solid.[11,18]

As noted, a variety of different spectra of nominally identical solid glycine samples have been published. However, even when made from nominally identical powders, spectra were shown to vary greatly, likely due to glycine forming large crystals extremely readily leading to linear dichroism.[11] Highly polycrystalline samples are preferred as otherwise the x-ray experiment may probe only one orientation of the crystal. Linear dichroism problems can also be minimized in certain cases using circularly polarized light. Some differences were tentatively

assigned to defects in the samples resulting in some neutral glycine molecule impurities, and to an inability to sample truly random orientations. Water can play a large role in changing the spectrum of amino acids.[30] Other causes could be radiation damage and interactions with adsorbed water.[17]

Simulating the spectrum of a solid can be challenging because of the number of atoms involved. However, several groups have made serious efforts toward accurately predicting the spectrum of crystalline glycine. One study explicitly calculated the spectrum of methylamine and methylamine hydrochloride in the presence of a full core hole (FCH) (used to model the resonant x-ray excitation) for both the isolated molecules and for clusters using the Hartree-Fock approximation to the electronic Hamiltonian, in an attempt to model the nitrogen edges of glycine(s) in its NH_2 and NH_3^+ charge states.[11] The clusters were modeled after the crystals. While this work is certainly informative and explains some of the underlying causes of the observed spectra, the authors clearly elaborate on the weaknesses of their approach. First, although they are modeling a system designed to explain the glycine(s) spectrum, they aren't actually modeling glycine, so it is hard to assess the accuracy of these results. They also numerically convolute their simulated spectra using a broad empirical linewidth and, although such an approach is common, it often obscures the spectral features, and its use is not adequately justified in the literature. The only thorough attempt to directly simulate the spectrum of solid glycine was undertaken using a multiple scattering code.[17] In that work, a cluster of 15 glycine molecules was simulated with a Debye-Waller factor of $0.01 Å^2$ to account for thermal vibrations. While the correct general spectral form is reproduced, it comprises unrealistically sharp features, similar to those found in sodium glycinate(s) before the main peak. This could be due to the difficulties in using multiple scattering methods to simulate low-Z elements such as hydrogen.[31]

Previous work has shown that density functional theory (DFT) [32,33] can accurately reproduce the excitation energies associated with core-level spectra via total energy differences (ΔSCF or ΔKS).[34] We model the lowest energy core-level state self-consistently with a full core hole and an associated excited electron (XCH).[35] This differs from the previously described FCH approximation, which ignores the excited electron and its screening effects entirely, or replaces it with a uniform background charge density (in the case of periodic systems).[36] Others have applied multielectron quantum chemistry to small, finite, single molecule systems, but generally these methods scale poorly with system size and would be far too expensive for the molecular dynamics sampling performed in this work.[37] Because the antibonding orbitals and Rydberg states probed by NEXAFS can be quite spatially extended,[19] they are sensitive to interactions over a considerable distance from the probed atom. We have chosen to use a plane wave representation of the electronic structure, capable of describing both localized and scattering states.[38]

Past research has attempted to simulate crystalline glycine NEXAFS spectra using the crystal structure with static nuclear coordinates, and perhaps including the effects of nuclear motion via the Debye-Waller factors. This frozen nuclei approach has often proved to be inadequate in the gas and liquid state,[38-40] as it neglects the impact of nuclear motion on the electronic transition amplitude in addition to the associated transition energy; to first order, this is referred to as the Herzberg-Teller effect.[38] Therefore, we attempted to simulate solid glycine as a crystal at various experimental temperatures by using molecular dynamics (MD) sampling to accurately represent thermal nuclear motion and associated variations in molecular conformations. Herein, we investigate the changes in the NEXAFS nitrogen K-edge spectrum of solid glycine, using MD sampling as a function of temperature, and make an explicit attempt to

account for the vibrations of the molecules.[41] We average over polarization directions to model a multicrystalline sample. We find that temperature variations have a significant impact on the spectrum of glycine(s).

2. Computational Methods

Our method for computing core-level spectra has been detailed previously.[35,38-40] Briefly, we calculate the absorption cross section to first order using Fermi's golden rule, with density functional theory (DFT) using the Perdew-Burke-Ernzerhof (PBE) form of the generalized-gradient approximation to the exchange-correlation potential.[42] We adopt a plane-wave representation and pseudopotential approximation for valence electronic structure, with norm-conserving pseudopotentials and a numerically converged plane-wave cut-off of 85 Rydberg.

We adopt the eXcited state Core Hole (XCH) approximation. For x-ray core hole excitations, the intial state is fixed on the 1s atomic eigenstate of interest and we include the important screening presence of the excited electron; in the atomic case the excited nitrogen has the electronic configuration $1s^1 2s^2 2p^4$. Because the atomic nuclei will not move appreciably on the attosecond time scale of the excitation, we consider them fixed in place during this process. We used approximately 1000 Kohn-Sham eigenstates in constructing transition matrix elements, which is sufficient to extend the transitions approximately 25 eV above the absorption onset. The electronic structure is calculated using the Quantum-ESPRESSO code.[43] We exploit periodic boundary conditions to approximate the continuum of electronic states found at high energy by numerically converging an integration over the first Brillouin Zone (BZ) with respect to the electronic wave vector k. These delocalized states are similar to the unbound electronic scattering states of the molecule. Spectra were shifted to match room temperature experimental

absorption onset energies, and different temperatures aligned to each other using total energy differences, as previously described.[39] A total of 125 k-points were used per spectra.[39]

Generally, core-level spectra of solids are simulated based on the crystal structure, usually determined by x-ray or neutron diffraction. The most stable structure and the one used in this work is α-glycine.[29] The crystal unit cell was repeated 4 times to produce a 16 molecule supercell, thus minimizing interactions between core-hole excitations on individual glycine molecules. This structure was then relaxed both with respect to inter- and intramolecular forces and stress on the crystal by modeling the atomic nuclei as fixed point charges, located at an energy minimum derived from a formalism which models the electrons as quantum particles and the nuclei as classical point charges. We performed this calculation on solid glycine and this result is referred to herein as 0 K calculations for simulating the x-ray absorption spectrum.

In order to account for the thermal motions, we have modeled the nuclear degrees of freedom in these molecules using molecular dynamics (MD) performed at the specified temperature, ranging from 77K to 450K using a Langevin thermostat in the NVT ensemble and the generalized AMBER force field.[44,45] Not surprisingly, given the relatively temperature invariant unit-cell parameters, despite using the same lattice parameters (constant volume) the pressure remained relatively constant with temperature.[29] The resulting distribution of nuclear coordinates were sampled at 1 nanosecond intervals (at least) to eliminate correlation between snapshots for 10 snapshots.[44,45] All nitrogen atoms in a given snapshot were sampled.

All calculated core-level transitions are numerically broadened using Gaussians of 0.2 eV full width at half maximum (FWHM). We use this relatively small and uniform broadening scheme with the aim of simulating and distinguishing electronic and vibrational effects explicitly. Certain broad features in the spectra result from the fundamental energy dispersion of

8

electronic states or the short lifetime of particular transitions, while other features will be caused by molecular motions.[19,38]   Using a small broadening permits a predictive computational approach which can distinguish between electronic broadening and vibrational broadening of spectral features.

Results and Discussion

Solid glycine in its most stable form (α-glycine) is a zwitterionic ($NH_3^+CH_2COO^-$) monoclinic crystal of space group $P2_1/n$.[44] Its crystal structure is relatively invariant with temperature until it decomposes at ~500K and there are several hydrogen bonds within the crystal.[29] An image of 4 units of the crystal structure is shown in Figure 1, as is the structure of zwitterionic glycine. This is the supercell size that was used to simulate the N K-edge spectra of glycine(s) in our calculations. In this figure, several hydrogen bonds are clearly visible between the nitrogen-containing amine group and the carboxylate group.

In order to ascertain the effect of temperature on the crystal, the crystal's internal degrees of freedom were simulated using molecular dynamics at several different temperatures. As the crystal temperature is increased, the internal degrees of freedom of the glycine molecules within a crystal rotate more freely.   This is evidenced by following the carbon-carbon-nitrogen-hydrogen dihedral angle, as is shown in Figure 2 part a. While there is always a significant barrier to rotation, at higher temperatures the spread of angles which are accessible is significantly larger than that at 77K. There are three major peaks at every temperature because the amine group, NH_3^+, has three hydrogens. In Figure 2 Part b, we provide a histogram of nitrogen-carbon-carbon-oxygen dihedral angle for glycine as a function of temperature. There are two major peaks at every temperature because the carboxylate group, CO_2^-, has 2 oxygen atoms. Again, the dihedral angle spread increases with temperature.

The calculated NEXAFS spectrum as a function of temperature is shown in Figure 3. The results are compared to the measured room temperature spectrum (~300 K).[17,22] The calculated nitrogen K-edge spectra of solid glycine at 0K, 77K, 198K, 300K and 450K are shown. The spectral changes are due to conformational changes of glycine, as all the molecules are simulated using the same crystal lattice parameters (constant volume). It is interesting to watch the evolution of the structure as a function of temperature. At 0K, the structure of all the glycine(s) molecules are identical, and this causes a spectrum with very well resolved features, unlike what is found experimentally at room temperature with most molecular solids. There are two well-resolved features below 405 eV, a large one at 406 eV and other smaller higher energy features. Upon heating the sample to 77K, the features below 405 eV merge together and the features above 405 eV merge together, giving a two-peaked spectrum with a large intensity gap at approximately 405 eV. The spectrum is not smooth however, as both peaks have substructures.

When glycine(s) is simulated at 198K, the spectrum is similar to that of the 77K spectrum. The spectral features blend together slightly more and the spectrum generally is smoother compared to the 77K spectrum. By 300K the spectrum comprises only a single large feature. This is the spectrum which can be directly compared to experiment, and although it is slightly contracted compared to the measurements (we believe due to DFT underestimating the bandwidth)[46] the spectra are quite similar. This is more surprising considering that the transitions were only broadened by 0.2 eV FWHM Gaussians, meaning that there are many transitions which comprise the spectrum. The continuum is slightly too weak relative to experiment, but this is not surprising, given that we do not account for multielectron excitations. The spectrum appears to acquire its form due to the thermal motions of the molecule, not from an inherent peak

width. The spectrum at 450K is similar to that of the 300K spectrum, with a noticeable redshift of approximately 1 eV. Glycine(s) begins to decompose at ~500K, meaning that measurements well above 450K will not be experimentally feasible.

Unfortunately, there is no simple relationship between the intramolecular dihedral angles and the calculated spectra. This is shown in Figure 4, which compares the nitrogen K-edge spectra versus the carbon-carbon-nitrogen-hydrogen dihedral angle (for the angle found between 0° and 120°) at 300K. As can be seen, there is much variation in the spectral intensity and it does not necessarily correlate simply with the dihedral angle. Similar phenomena are observed with other angles, distances and temperatures, i.e., we have found no simple relationship between any simple structural variable and the spectra, including making and breaking of hydrogen bonds with other glycine(s) molecules. Given the relatively strong spectral correlation with the nitrogen-carbon-carbon-oxygen bond angle found in the gas phase, it is notable that there is no simple relationship between that bond angle either and the spectrum.[38] It is important to realize that these changes associated with the different locations of the atoms appear to be the major cause of the spectral structure. Even with use of a small numerical broadening it is still possible to generate a spectrum at room temperature which matches experiment and we can conclude that this is due to the large thermal motions of the molecule. It would be a worthwhile future goal for x-ray absorption theorists to correlate the position of atoms (possibly via a normal mode analysis) with spectral peak positions and intensities. Another viable option is using phonon coupling.[47] The importance of conformation in gas phase amino acids has been examined experimentally by XPS and x-ray absorption.[12,48,49]

It has occasionally been difficult to reproduce spectra of solid glycine, even under nominally identical conditions.[4,11,15-18] While early spectral inconsistencies could have been due

to sample preparation techniques, previous experiments supported the notion that linear dichroism could be a source of irreproducibility; however, our calculations on the nitrogen K-edge indicate that this effect is limited.[11] In particular, new techniques avoid this problem by sampling a variety of crystalline domains.[17] In our calculations, it only takes on the order of 100 glycine(s) spectra to converge the solid glycine nitrogen K-edge spectrum, implying that avoiding insufficient crystal sampling should be readily achievable. However, other effects such as crystalline domain shifts and neutral glycine impurities could produce significant effects on the spectra. Furthermore, it is known that these crystals may contain water impurities, which could affect the spectra.[8] Crystal damage and x-ray induced chemical effects should be less problematic due to new experimental techniques.[17]

4. Conclusion

Nitrogen K-edge NEXAFS spectra of solid glycine have been calculated as a function of temperature, ranging from 0 K to approaching the decomposition temperature. It was found that the thermal motions induce large spectral variations, and that these intramolecular motions actually define the spectrum that is observed at room temperature. The room temperature spectrum, which comprises just one large peak, is not due to an inherently broad peak structure, but rather, to the thermal motions of the molecule. These motions cannot be described by a single simple structural variable, but rather are due to collective motions throughout the crystal. Obtaining a temperature dependent spectrum of solid glycine is a worthwhile goal for experimentalists as a way of quantifying the importance of molecular motions.

Acknowledgements

Figure and Table Captions

Figure 1. Part a) is an image of two units of the most stable crystal structure of glycine, with oxygen in red, carbon in pale blue, nitrogen in blue and hydrogen in teal. Several hydrogen bonds are visible as block dotted lines between the amine group and the carboxylate group. The unit-cell is shown. Part b) is the structure of an individual zwitterionic glycine molecule.

Figure 2. Part a) is a histogram of carbon-carbon-nitrogen-hydrogen dihedral angle for glycine as a function of temperature. As temperature increases, the spread in values increases. There are three major peaks at every temperature because the amine group, NH_3^+, has 3 hydrogen atoms. Part b) is a histogram of nitrogen-carbon-carbon-oxygen dihedral angle for glycine as a function of temperature. As temperature increases, the spread in values increases. There are two major peaks at every temperature because the carboxylate group, CO_2^-, has 2 oxygen atoms.

Figure 3. The calculated spectra of solid glycine at various temperatures ranging from 0K to 450K at the nitrogen K-edge. For all temperatures besides 0K, the shaded region represents 1 standard deviation. The spectra are compared with a room temperature spectrum from the literature (see text). Spectra are offset for clarity

Figure 4. Individual calculated nitrogen K-edge NEXAFS spectra plotted as a function of carbon-carbon-nitrogen-hydrogen dihedral angle, for the angle found between 0° and 120° at 300K.
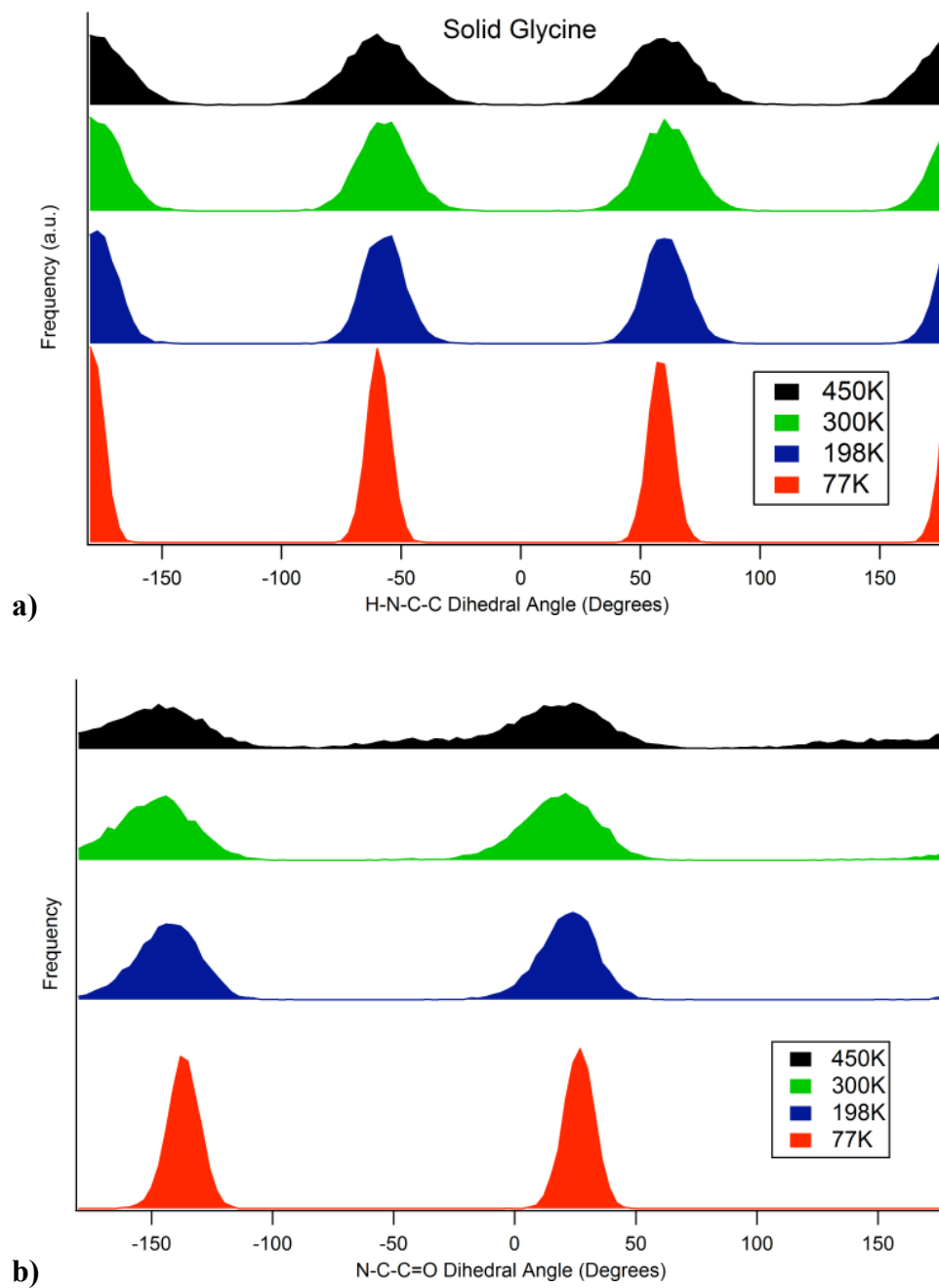
Figures and Tables
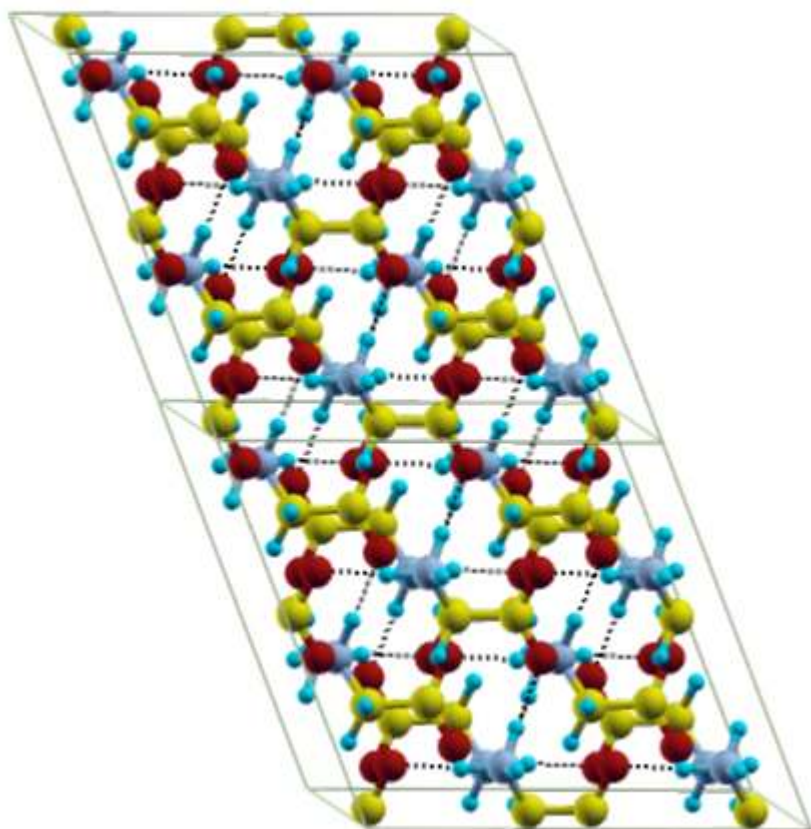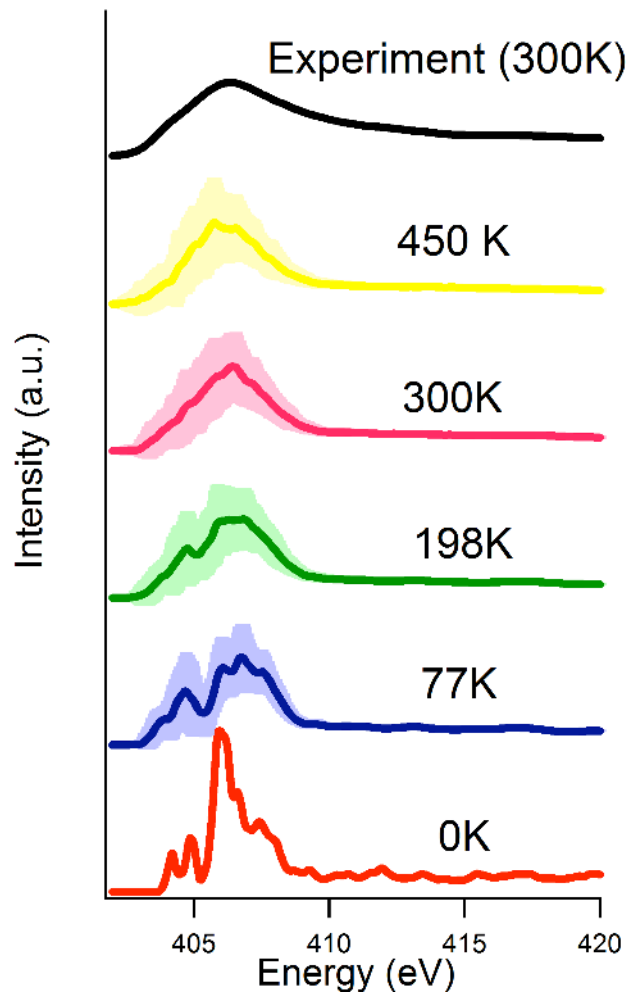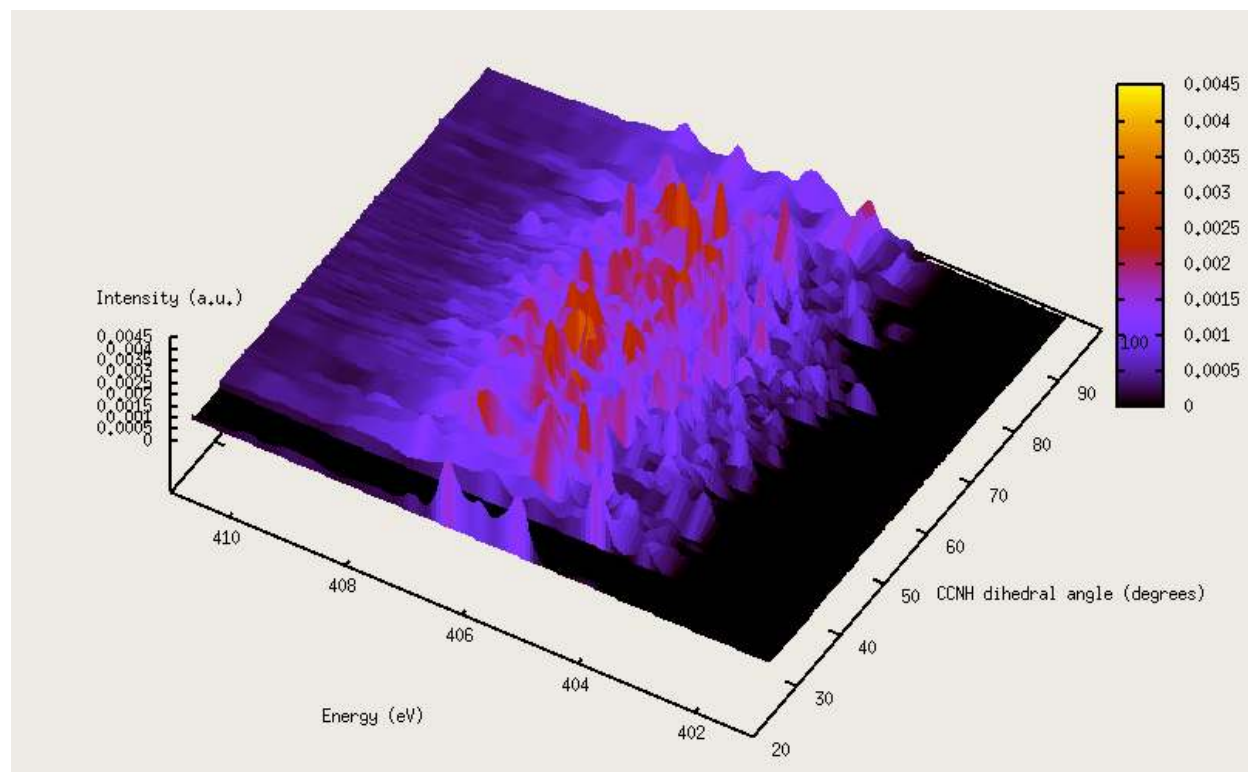

a)
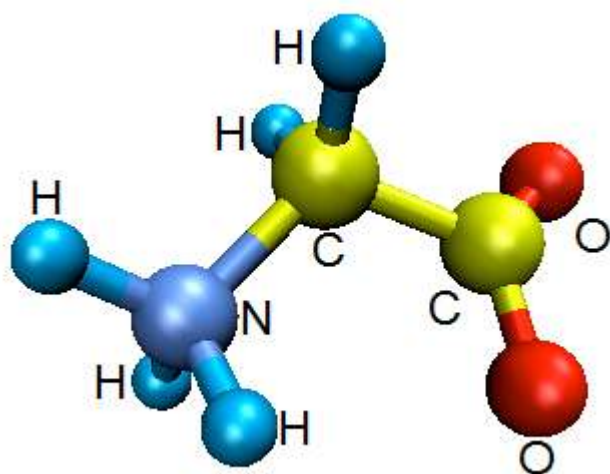
b)

Figure 1

Figure 2

Figure 3

Figure 4

1   V. Carravetta, O. Plashkevych, and H. Agren, Journal of Chemical Physics **109** (4), 1456 (1998).

2   V. Feyer, O. Plekan, T. Skala, V. Chab, V. Matolin, and K. C. Prince, Journal of Physical Chemistry B **112** (43), 13655 (2008).

3   V. Feyer, O. Plekan, R. Richter, M. Coreno, K. C. Prince, and V. Carravetta, Journal of Physical Chemistry A **112** (34), 7806 (2008).

4   M. L. Gordon, G. Cooper, C. Morin, T. Araki, C. C. Turci, K. Kaznatcheev, and A. P. Hitchcock, Journal of Physical Chemistry A **107** (32), 6144 (2003).

5   J. Hasselstrom, O. Karis, M. Weinelt, N. Wassdahl, A. Nilsson, M. Nyberg, L. G. M. Pettersson, M. G. Samant, and J. Stohr, Surface Science **407** (1-3), 221 (1998).

6   K. Kaznacheyev, A. Osanna, C. Jacobsen, O. Plashkevych, O. Vahtras, and H. Agren, Journal of Physical Chemistry A **106** (13), 3153 (2002).

7   B. M. Messer, C. D. Cappa, J. D. Smith, W. S. Drisdell, C. P. Schwartz, R. C. Cohen, and R. J. Saykally, Journal of Physical Chemistry B **109** (46), 21640 (2005).

8   B. M. Messer, C. D. Cappa, J. D. Smith, K. R. Wilson, M. K. Gilles, R. C. Cohen, and R. J. Saykally, Journal of Physical Chemistry B **109** (11), 5375 (2005).

9   M. Nyberg, J. Hasselstrom, O. Karis, N. Wassdahl, M. Weinelt, A. Nilsson, and L. G. M. Pettersson, Journal of Chemical Physics **112** (12), 5420 (2000).

10 M. Nyberg, M. Odelius, A. Nilsson, and L. G. M. Pettersson, Journal of Chemical Physics **119** (23), 12577 (2003).

11 E. Otero and S. G. Urquhart, Journal of Physical Chemistry A **110** (44), 12121 (2006).

12 O. Plekan, V. Feyer, R. Richter, M. Coreno, M. de Simone, K. C. Prince, and V. Carravetta, Journal of Electron Spectroscopy and Related Phenomena **155** (1-3), 47 (2007).

13 M. Tanaka, K. Nakagawa, T. Koketsu, A. Agui, and A. Yokoya, Journal of Synchrotron Radiation **8**, 1009 (2001).

14 L. Yang, O. Plashkevych, O. Vahtras, V. Carravetta, and H. Agren, Journal of Synchrotron Radiation **6**, 708 (1999).

15 Y. Zubavichus, M. Zharnikov, A. Schaporenko, and M. Grunze, Journal of Electron Spectroscopy and Related Phenomena **134** (1), 25 (2004).

16 Y. Zubavichus, A. Shaporenko, M. Grunze, and M. Zharnikov, Journal of Physical Chemistry A **109** (32), 6998 (2005).

17 Y. Zubavichus, A. Shaporenko, M. Grunze, and M. Zharnikov, Journal of Physical Chemistry B **110** (7), 3420 (2006).

18 G. Cooper, M. Gordon, D. Tulumello, C. Turci, K. Kaznatcheev, and A. R. Hitchcock, Journal of Electron Spectroscopy and Related Phenomena **137-40**, 795 (2004).

19 J. Stöhr, *NEXAFS Spectroscopy*. (Springer, Berlin, 1992).

20 Y. Zubavichus, A. Shaporenko, M. Grunze, and M. Zharnikov, Journal of Physical Chemistry B **112** (15), 4478 (2008).

21 Y. Zubavichus, A. Shaporenko, M. Grunze, and M. Zharnikov, Journal of Physical Chemistry B **111** (40), 11866 (2007).

22 J. Stewart-Ornstein, A. P. Hitchcock, D. H. Cruz, P. Henklein, J. Overhage, K. Hilpert, J. D. Hale, and R. E. W. Hancock, Journal of Physical Chemistry B **111** (26), 7691 (2007).

23 G. Albrecht and R. B. Corey, Journal of the American Chemical Society **61**, 1087 (1939).

24 J. Almlof, A. Kvick, and J. O. Thomas, Journal of Chemical Physics **59** (8), 3901 (1973).

25 P. G. Jonsson and A. Kvick, Acta Crystallographica Section B-Structural Crystallography and Crystal Chemistry **B 28** (6), 1827 (1972).

26 J. P. Legros and A. Kvick, Acta Crystallographica Section B-Structural Science **36** (DEC), 3052 (1980).

27 A. Peeters, C. Vanalsenoy, A. T. H. Lenstra, and H. J. Geise, Journal of Chemical Physics **103** (15), 6608 (1995).

28 L. F. Power, K. E. Turner, and F. H. Moore, Acta Crystallographica Section B-Structural Science **32** (JAN15), 11 (1976).

29 P. Langan, S. A. Mason, D. Myles, and B. P. Schoenborn, Acta Crystallographica Section B-Structural Science **58**, 728 (2002).

30 D. Nolting, E. F. Aziz, N. Ottosson, M. Faubel, I. V. Hertel, and B. Winter, Journal of the American Chemical Society **129** (45), 14068 (2007).

31 J. J. Rehr and A. L. Ankudinov, Coordination Chemistry Reviews **249** (1-2), 131 (2005).

32 P. Hohenberg and W. Kohn, Physical Review B **136** (3B), B864 (1964).

33 W. Kohn and L. J. Sham, Physical Review **140** (4A), 1133 (1965).

34 C. Kolczewski, R. Puttner, O. Plashkevych, H. Agren, V. Staemmler, M. Martins, G. Snell, A. S. Schlachter, M. Sant'Anna, G. Kaindl, and L. G. M. Pettersson, Journal of Chemical Physics **115** (14), 6426 (2001).

35 D. Prendergast and G. Galli, Physical Review Letters **96** (21) (2006).

36 Y. Luo, H. Agren, M. Keil, R. Friedlein, and W. R. Salaneck, Chemical Physics Letters **337** (1-3), 176 (2001).

37 D. Duflot, K. Sidhoum, J. P. Flament, A. Giuliani, J. Heinesch, and M. J. Hubin-Franskin, European Physical Journal D **35** (2), 239 (2005).

38 J. S. Uejio, C. P. Schwartz, R. J. Saykally, and D. Prendergast, Chemical Physics Letters **467** (1-3), 195 (2008).

39 C. P. Schwartz, J. S. Uejio, R. J. Saykally, and D. Prendergast, Journal of Chemical Physics **130** (18) (2009).

40 C. P. Schwartz, J. S. Uejio, A. M. Duffin, A. H. England, D. Prendergast, and R. J. Saykally, Journal of Chemical Physics **131** (11) (2009).

41 C. Chakravarty, International Reviews in Physical Chemistry **16** (4), 421 (1997).

42 J. P. Perdew, K. Burke, and M. Ernzerhof, Physical Review Letters **77** (18), 3865 (1996).

43 P. Giannozzi, S. Baroni, N. Bonini, M. Calandra, R. Car, C. Cavazzoni, D. Ceresoli, G. L. Chiarotti, M. Cococcioni, I. Dabo, A. Dal Corso, S. de Gironcoli, S. Fabris, G. Fratesi, R. Gebauer, U. Gerstmann, C. Gougoussis, A. Kokalj, M. Lazzeri, L. Martin-Samos, N. Marzari, F. Mauri, R. Mazzarello, S. Paolini, A. Pasquarello, L. Paulatto, C. Sbraccia, S. Scandolo, G. Sclauzero, A. P. Seitsonen, A. Smogunov, P. Umari, and R. M. Wentzcovitch, Journal of Physics-Condensed Matter **21** (39) (2009).

44 T. A. D. D.A. Case, T.E. Cheatham, III, C.L. Simmerling, J. Wang, R.E. Duke, R., K. M. M. Luo, D.A. Pearlman, M. Crowley, R.C. Walker, W. Zhang, B. Wang, S., A. R. Hayik, G. Seabra, K.F. Wong, F. Paesani, X. Wu, S. Brozell, V. Tsui, H., L. Y. Gohlke, C. Tan, J. Mongan, V. Hornak, G. Cui, P. Beroza, D.H. Mathews, C., and W. S. R. Schafmeister, and P.A. Kollman, (2006).

45 J. M. Wang, W. Wang, P. A. Kollman, and D. A. Case, Journal of Molecular Graphics & Modelling **25** (2), 247 (2006).

46   D. Prendergast, J. C. Grossman, and G. Galli, Journal of Chemical Physics **123** (1) (2005).
47   C. Brouder, D. Cabaret, A. Juhin, and P. Sainctavit, Physical Review B **81** (11).
48   O. Plekan, V. Feyer, R. Richter, M. Coreno, M. de Simone, K. C. Prince, and V. Carravetta, Chemical Physics Letters **442** (4-6), 429 (2007).
49   O. Plekan, V. Feyer, R. Richter, M. Coreno, M. de Simone, K. C. Prince, and V. Carravetta, Journal of Physical Chemistry A **111** (43), 10998 (2007).